ER45072-49

Surface Structure and Spectroscopy of Charge-Density Wave Materials Using Scanning Tunneling Microscopy

by

R.V. Coleman, Zhenxi Dai, W.W. McNairy

C.G. Slough and Chen Wang

Department of Physics

University of Virginia

Charlottesville, VA 22901 U.S.A.

DOE/ER/45072--49

DE92 007746

The Scanning tunneling microscope (STM) has been used to study the effects of Fe doping on the charge-density wave (CDW) structure in $NbSe_3$ and 1T-TaS_2. In $NbSe_3$ small amounts of Fe reduce both CDW gaps by 25-30% and change the relative CDW amplitudes of the high and low temperature CDWs. The CDW amlplitudes remain strong on all three chains of the surface unit cell with no evident disorder. In 1T-$Fe_{0.05}Ta_{0.95}S_2$ the Fe introduces substantial disorder in the CDW pattern, but the local CDW amplitude remains strong. The CDW energy gap is reduced by approximately 50% and the resistive anomaly at the commensurate-incommensurate transition is removed. The STM in both the image and spectroscopy modes can detect subtle changes in CDW structure due to impurities.

DISCLAIMER

I. INTRODUCTION

We have used scanning tunneling microscopes (STMs) operating at cryogenic and room temperatures to image the surface structure of charge density waves (CDWs), and to measure CDW energy gaps in transition metal dichalcogenides [1] and trichalcogenides [2]. The formation of CDWs is accompanied by a modification of the local density of states (LDOS) to which the STM is directly sensitive. The magnitude of the CDW z-deflection can be directly related to the strength of the CDW in the material. In the pure state, the transiton metal dichalcogenides and trichalcogenides show a broad range of transition temperatures and CDW strengths and are thus ideal specimens for study with the STM [3]. Doping of the pure crystals with impurities such as Fe can be expected to produce changes in the CDW structure which may be detected in both the STM images and in spectroscopic curves.

In the spectroscopic mode the STM can be used to detect changes in the energy gap structure of CDW compounds. We have studied CDW compounds in which the Fermi surface (FS) gapping ranges from a small fraction of the FS to complete gapping of the FS. Therefore, in many cases a subtantial density of states (DOS) exists at the Fermi level, and the magnitude of the conductance change at the gap edge is quite variable for different compounds. The presence of CDW gaps introduces changes of slope in the I versus V and peaks in the dI/dV versus V characteristic curves. A systematic study [4,5] of the CDW gap structure in chalcogenides, which have a large range of gap values, yields a consistent set of data. Measurements of CDW gaps with the STM are straightforward, but the geometry of a sharp tip located near an atomically flat surface makes the junction extremely sensitive to tunneling anomalies. For example, the presence of zero bias anomalies (ZBAs) complicates the analysis of the spectroscopic curves. However, we believe that most ZBAs are associated with particular crystal-tip combinations, and crystal-tip combinations can be found for which ZBAs are not present.

In this paper we compare STM data obtained on pure $NbSe_3$ and on $NbSe_3$ doped with

dilute Fe impurities [6]. We also report STM data on 1T-$Fe_{0.05}Ta_{0.95}S_2$. Analysis of spectroscopic curves for Fe doped $NbSe_3$ show that the gap structure is rapidly modified by the presence of small amounts of Fe. At the higher Fe concentration present in 1T-$Fe_{0.05}Ta_{0.95}S_2$ disorder in the CDW structure can be is observed in the STM images. For $Fe_{0.01}NbSe_3$ the STM images indicate that changes have occured in the realtive amplitudes of the two CDWs in $NbSe_3$. In both Fe doped crystals, the local CDW amplitude remains extremely strong.

II. EXPERIMENTAL TECHNIQUES

The transition metal dichalcogenides were grown by the method of iodine vapour transport. Stochiometric quanties of powder were sealed in quartz tubes and sintered at ~900 °C. The tubes are then placed in an oven set to the correct temperature for the compound and phase desired. For example, the pure 1T phase TaS_2 crystals were grown at temperatures above 900 °C in a gradient of 10 °C/in. for several weeks. These crystals are also quenched from high temperature to room temperature where the 1T phase is stable indefinitely. Pure and doped $NbSe_3$ crystals were also grown from sintered powders at 750 °C in a gradient of 25 °C/in. for one to three weeks.

The crystals were cleaved in air before mounting on the STM (some as-grown surfaces of the trichalcogenides also give good images). For data taken at 4.2 or 77 K the microscope is placed in a chamber which is evacuated and back filled with helium or nitrogen gas before immersing the STM in the liquid. Surface adsorption is very limited under this procedure. At room temperature the microscope can be operated in He or N_2 gas. The tips used in both the imaging and spectroscopic modes were machined from 99.9% pure $Pt_{0.8}Ir_{0.2}$ wire.

All STM images presented here were taken in the constant current mode. I versus V curves were recorded by briefly disconnecting the feedback signal to the microscope and sweeping the voltage. Conductance curves were recorded with a lock-in amplifier using the

standard AC modulation technique.

III. RESULTS AND DISCUSSION

A. $NbSe_3$ and $Fe_{0.01}NbSe_3$

$NbSe_3$ is a quasi-one dimensional linear chain compound which grows in a monoclinic phase. There are six trigonal chains per unit cell. A cross section of the unit cell perpendicular to the chain axis (b-axis) is shown in Fig. 1. Each chain consists of prismatic cages of six Se atoms with a Nb atom located near the center of the cage. The six chains form three pairs of electronically and structurally inequivalent chains denoted I,I′, II,II′ and III,III′ in the band structure calculation by Shima and Kamimura [7]. $NbSe_3$ undergoes two CDW transitions with onset temperatures of 145 and 59 K. The CDWs remain incommensurate down to the lowest temperatures measured. The 145 K transition is associated with the pair of chains denoted III, III′ and has a wavelength of $(0a_0, 4.115b_0, 0c_0)$. The low temperature CDW wavelength is $(2.00a_0, 3.802b_0, 2.00c_0)$. A conjecture by Wilson [8] suggested that the low temperature CDW was confined to chains I,I′, while chains II,II′ carry little or no electron density. Initial NMR results by Wada, Aoki, and Fujita [9], and by Devreux [10], tended to support these conclusions. However, more recent NMR results by Shi and Ross [11] suggest substantial conduction electron density on chains II and II′.

The STM images, which measure the LDOS at the position of the tip, detect a substantial CDW modulation on all three chains [12], as shown in Fig. 2. The low temperature CDW modulation appears on chains I′ and II with approximately equal amplitude. This is not inconsistent with the detailed band structure calculations of Shima and Kamimura [7] in which Fermi surface sections derived from wave functions of both chains I′ and II form the low temperature CDW. The modulations on chains I′ and II, as identified in Fig. 2, alternate phase by 180° between adjacent unit cells as expected for the low temperature CDW. The high temperature CDW on chain III remains in phase across adjacent unit cells, and is more

localized. As shown in Fig. 3, the STM profiles show the correct wavelength relation between the low temperature and high temperature CDW.

Figure 4(a) is a STM grey scale scan of $Fe_{0.01}NbSe_3$ obtained at 4.2 K. As with the image of the pure material, all three chains of the surface unit cell show a charge modulation. However, the relative amplitudes of the low temperature and high temperature CDWs are modified, with the high temperature CDW amplitude increased relative to that of the low temperature CDW. This is demonstrated in Fig. 4(b), which shows two profiles, one along chain III and one along chain I'.

Figure 5 shows conductance versus bias voltage curves obtained on pure $NbSe_3$ and on $Fe_{0.01}NbSe_3$ at 4.2 K. The conductance curve of the pure material shows clear evidence of two gaps situated at 35.0 ± 1.5 mV and at 101.0 ± 1.8 mV, which are identified with the low and high temperature CDWs respectively.

Figure 5(b) indicates that for the Fe doped material both gaps have been significantly reduced. The magnitudes for the low and high temperature CDW energy gaps are 24.8 ± 1.8 meV and 73.2 ± 1.1 meV respectively. This represents a 25-30% reduction from the values measured for the pure material. For the doped crystal the gap structure is enhanced for the high temperature CDW as compared to the pure crystal, indicating an increase in the LDOS change associated with the high temperature CDW gap. The above observations indicate that the dilute Fe doping has a major effect on the CDW potential and the FS nesting. The magnitudes of the CDW energy gaps are reduced, and this is accompanied by a relative increase in the high temperature CDW amplitude. This is consistent with the enhanced gap structure observed in the conductance curve of Fig. 5(b).

B. 1T-TaS_2 and 1T-$Fe_{0.05}Ta_{0.95}S_2$

1T-TaS_2 undergoes a CDW transition at an onset temperature of ~600 K. The CDW is defined by a triple-**q** structure, with **q** vectors rotated 120° from each other in the plane of

the sandwich. Initially, the CDW is incommensurate and aligned with the atomic lattice. Below ~350 K the CDW wavevector makes a discontinuous rotation to an angle of 11° with the atomic lattice, but remains imcommensurate. Between 350 K and 150 K the wavevector rotates to form various domain states, and at ~150 K becomes commensurate with an angle of 13.9°. Several incommensurate phases have been identified on warming and cooling between 350 K and 150 K, and have been studied with STM by several authors [13,14,15].

Figure 6 shows conductance versus bias voltage curves obtained on 1T-TaS_2 and 1T-$Fe_{0.05}Ta_{0.95}S_2$ at 4.2 K. The conductance versus bias curve for the pure material shows an approximately flat conductance up to ~150 mV, followed by a rapid rise beyond ~150 mV. We associate the onset of the rapid rise in conductance with the CDW gap edge. The value of $2\Delta_{CDW}/k_BT_c$ calculated from this measurement is 5.8.

The conductance curve obtained on the Fe alloy shows the gap has been reduced by a factor of ~2. Once again the conductance is relatively flat up to a voltage of ~50-75 mV, followed by a rapid rise beyond that value. Preliminary results indicate that this measurement is not a local phenomena, but can be obtained over the entire crystal. Comparison of STM scans on pure and Fe doped 1T-TaS_2 crystals show that the Fe introduces substantial disorder in the long range CDW structure. However, local CDW amplitudes remain strong. In addition, major changes in the resistance versus temperature curves are introduced [16] by the Fe.

IV. CONCLUSION

The STM image and spectroscopy data on $Fe_{0.01}NbSe_3$ and 1T-$Fe_{0.05}Ta_{0.95}S_2$ indicate that the Fe can induce major changes in the CDW structure. In the case of $Fe_{0.01}NbSe_3$ the final Fe concentration in the single crystal has been shown [6] to be reduced to the range of 0.1 to 0.01% compared to the starting amount of 1%. Even this small concentration substantially reduces the CDW energy gaps and changes the relative amplitude of the two

CDW charge modulations. However, in both the pure and Fe doped $NbSe_3$ the CDW amplitude modulation is strong on all three chains of the unit cell. The detailed FS nesting and CDW condensation appears to be extremely sensitive to Fe impurities even though little or no disorder is introduced.

In 1T-$Fe_{0.05}Ta_{0.95}S_2$ the final crystal retains ~5% Fe and the STM images show substantial disorder in the long range CDW pattern. However, on a local scale the CDW amplitude remains strong although the STM spectroscopy indicates a substantial reduction in the CDW energy gap from ~150 meV to ~75 meV.

Although both the Fe doped 1T-TaS_2 and the Fe doped $NbSe_3$ show substantial reductions in the CDW energy gaps, the basic effects on the CDW structure may be quite different. Fe doped $NbSe_3$ retains an ordered CDW structure and the resistance anomalies associated with the CDW are unchanged from those in the pure crystal. In 1T-TaS_2 the CDW resistive anomaly at ~150 K is eliminated and replaced by a rising resistance due to either magnetic scattering or electron localization [16]. The STM in both the imaging and spectroscopy mode can clearly be used for further detailed studies of impurity effects in CDW systems.

ACKNOWLEDGEMENTS

This work has been supported by the U.S. Department of Energy, Grant No. DOE-FG05-84ER45072. Useful discussions have been held with L.M. Falicov, R.E. Thomson, A. Zettl, V. Celli and P.K. Hansma.

REFERENCES

[1] J.A. Wilson, F.J. DiSalvo and S.J. Majahan, Adv. Phys. **24** (1975) 117.

[2] J.A. Wilson, Phys. Rev. B **19** (1979) 6456.

[3] R.V. Coleman, B. Giambattista, P.K. Hansma, A. Johnson, W.W. McNairy and C.G. Slough, Adv. Phys. **37** (1988) 559.

[4] Chen Wang, B. Giambattista, C.G. Slough, R.V. Coleman and M.A. Subramanian, Phys. Rev. B **42** (1990) 8890.

[5] Chen Wang, C.G. Slough and R.V. Coleman, J. Vac. Sci. Technol. B **9** (1991) 1048.

[6] R.V. Coleman, M.P. Everson, Hao-An Lu, A. Johnson and L.M. Falicov, Phys. Rev. B **41** (1990) 460.

[7] N. Shima and H. Kamimura in: Theoretical Aspects of Band Structures and Electronic Properties of Pseudo-One-Dimensional Solids, Ed. H. Kamimura (Reidel, Boston, 1985) p. 231.

[8] J.A. Wilson, J. Phys. F **12** (1982) 2469.

[9] Shinji Wada, Ryozo Aoki and Osamu Fujita, J. Phys. F **14** (1984) 1515.

[10] F. Devreux, J. Phys. (Paris) **43** (1982) 1489.

[11] Jianhui Shi and Joseph H. Ross, Jr. (to be published).

[12] Zhenxi Dai, C.G. Slough and R.V. Coleman, Phys. Rev. Lett. **66** (1991) 1318.

[13] R.E. Thomson, U. Walter, E. Ganz, J. Clarke, A. Zettl, P. Raunch and F.J. DiSalvo, Phys. Rev. B **38** (1988) 10734.

[14] C.G. Slough, W.W. McNairy, Chen Wang and R.V. Coleman, J. Vac. Sci. Technol. B **9** (1991) 1036.

[15] B. Burk, R.E. Thomson, A. Zettl and John Clark, Phys. Rev. Lett. **66** (1991) 3040.

[16] D.A. Whitney, R.M. Fleming and R.V. Coleman, Phys. Rev. B **15** (1977) 3405.

FIGURE CAPTIONS

Fig. 1. Cross section of $NbSe_3$ unit cell perpendicular to the chain axis (b-axis). The solid atoms lie in the plane of the figure and the open atoms are out of the plane. At the b-c plane surface there are three chains per unit cell; two are in-phase along the b-axis and one is displaced by $b_0/2$ from the two in-phase chains. The height variation of the surface Se atoms is 1.52 Å. The numbers indicate the negative charges on the Se atoms in the non-CDW phase. The chain designations as type I,I′, II,II′ and III,III′ follow the nomencalture used in Ref. 7.

Fig. 2. Grey scale STM scan of the b-c plane on $NbSe_3$ at 4.2 K. The high and low temperature CDWs are simultaneously resolved. The high temperature CDW on chain III is identified with the narrow charge modulation which remains in-phase across unit cells. The low temperature CDW is identified with the complex charge modulation on chains I′ and II. Note the modulations on each chain are out of phase and represent separate modulations located on chains I′ and II. Also note each of these modulations is out of phase across adjacent unit cells. The image was recorded with the scan direction making an angle of ~40° with the chain axis. (I = 2 nA, V = 50 mV). From Ref. 12.

Fig. 3. Profiles of z deflection for the high and low temperature CDWs on chains III and I′, respectively. The two modulations start in phase and continuously move out of phase, with the longer wavelength belonging to the high temperature CDW (upper curve). This is consistent with the incommensurate wavelengths of $4.115b_0$ for the high temperature CDW and $3.802b_0$ for the low temperature CDW as measured by x-ray diffraction. The amplitude of the CDW charge modulation on chain III is less than that observed on chains I′ and II. From Ref. 12.

Fig. 4.(a) Grey scale STM scan of the b-c plane on $Fe_{0.01}NbSe_3$ at 4.2 K. As in the image of the pure material, all three surface chains carry a strong charge modulation. (I = 2 nA, V = 50 mV). (b) Profiles of the z deflection for the high and low temperature CDWs on chains III and I′ respectively. The amplitude of the high temperature charge modulation on

chain III is now larger than the amplitude of the CDW charge modulation on chain I'.

Fig. 5.(a) Conductance versus bias voltage curve measured on $NbSe_3$ at 4.2 K. Structure in the conductance at voltages of ±35.0 mV and ±101 mV are identified with the low and high temperature CDW gaps respectively. (b) Conductance versus bias voltage curve measured on $Fe_{0.01}NbSe_3$ at 4.2 K. Structure which can be identified with the CDW gaps is also observed. However, the structure of the curves occurs at 24.8 mV and 73.2 mV, respectively. These voltages are 25-30% less than observed in pure $NbSe_3$.

Fig. 6. (a) Conductance versus bias voltage curve measured on 1T-$Fe_{0.05}Ta_{0.95}S_2$ at 4.2 K. A sharp increase in conductance at approximately ±50-75 mV is observed thereby indicating a reduction in the gap by a factor of ~2. (b) Conductance versus bias voltage curve measured on 1T-TaS_2 at 4.2 K. A sharp increase in conductance at ±150 mV can be identified with the CDW gap and the resulting change in DOS. From Ref. 5.

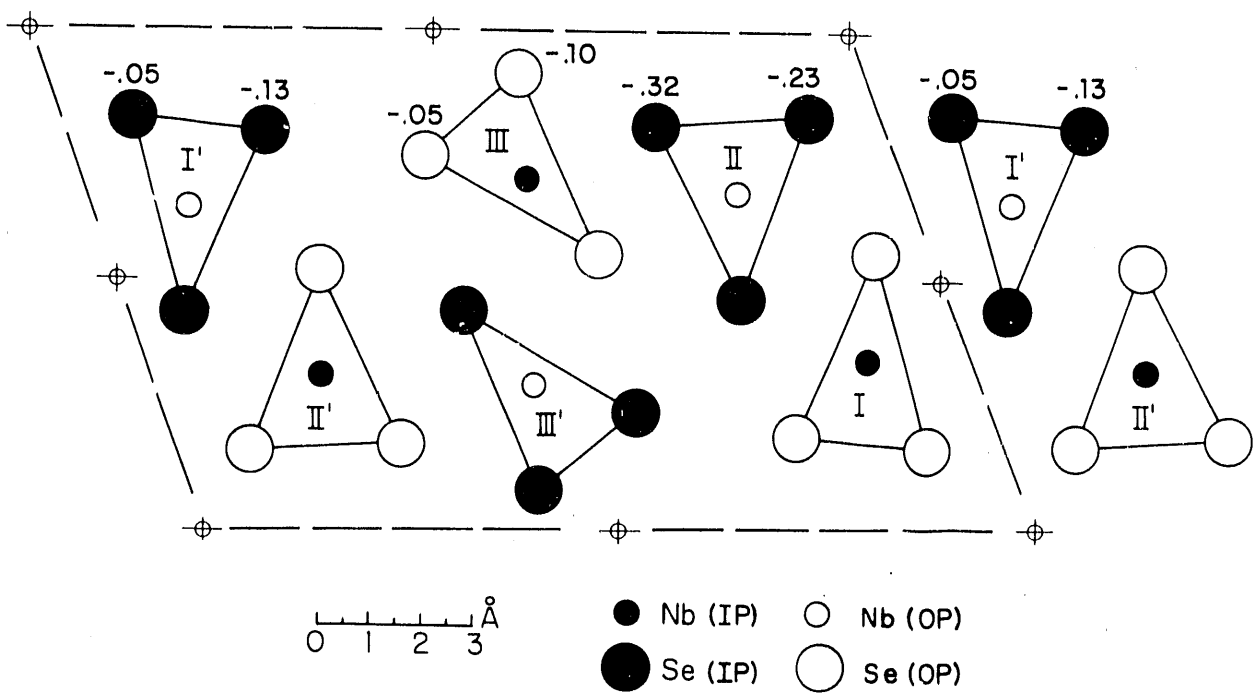
-.05
-.13
I'
-.10
-.05
III
-.32
-.23
II
-.05
-.13
I'
II'
III'
I
II'
0 1 2 3 Å
Nb (IP)
Nb (OP)
Se (IP)
Se (OP)

Fig. 1

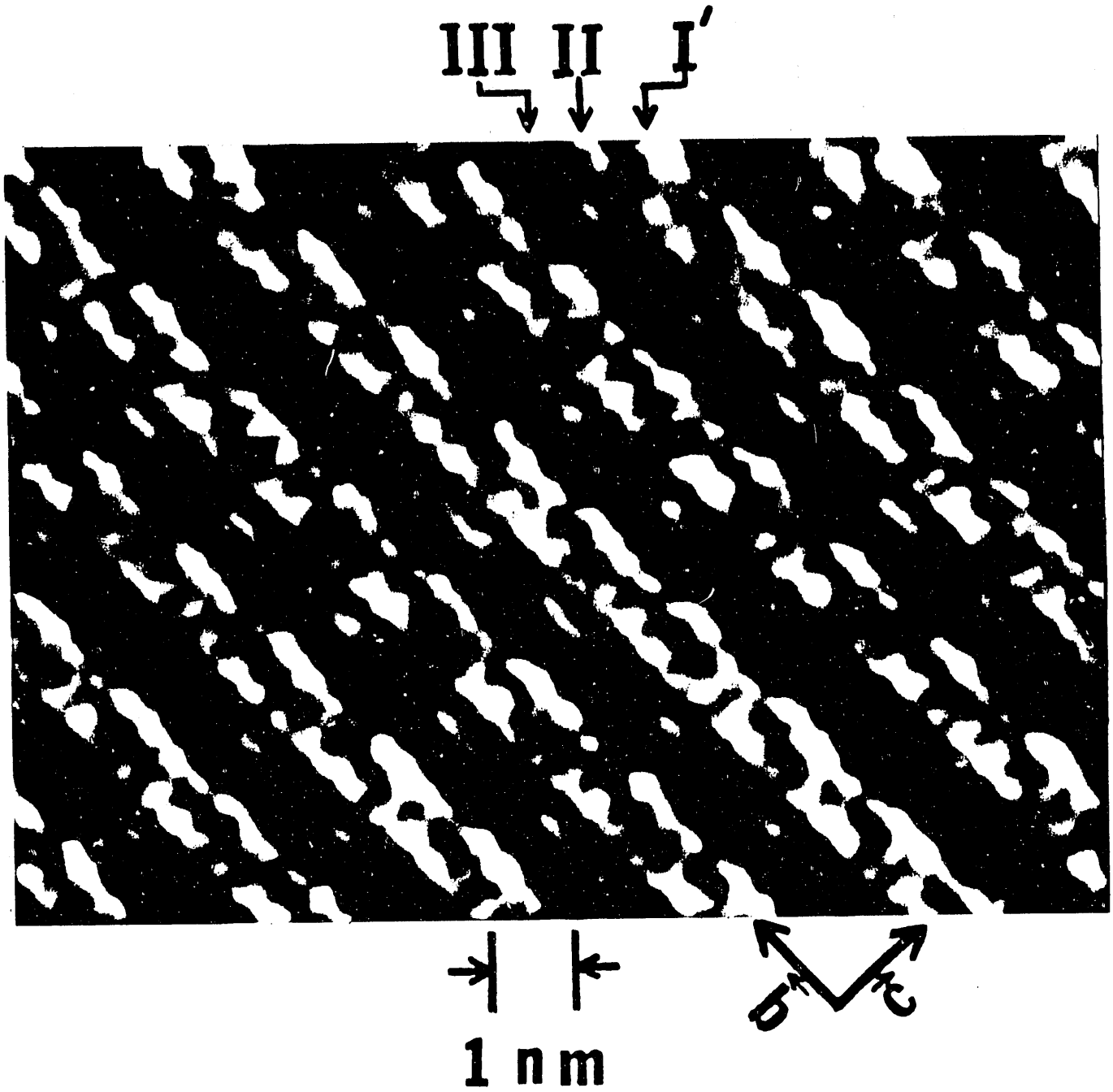

Fig. 2

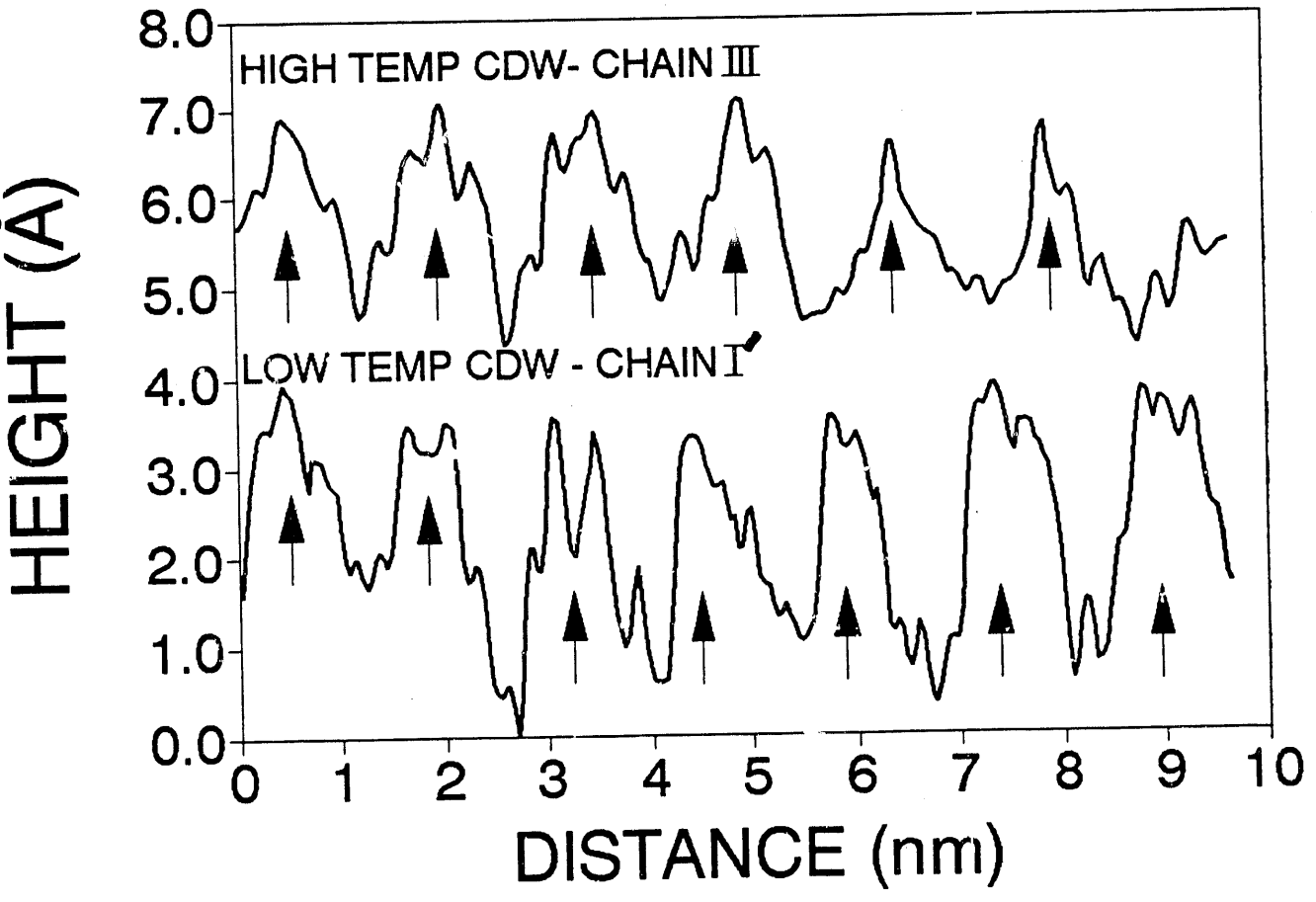
HEIGHT (Å)
8.0
7.0
6.0
5.0
4.0
3.0
2.0
1.0
0.0
HIGH TEMP CDW- CHAIN III
LOW TEMP CDW - CHAIN I
0
1
2
3
4
5
6
7
8
9
10
DISTANCE (nm)

Fig. 3

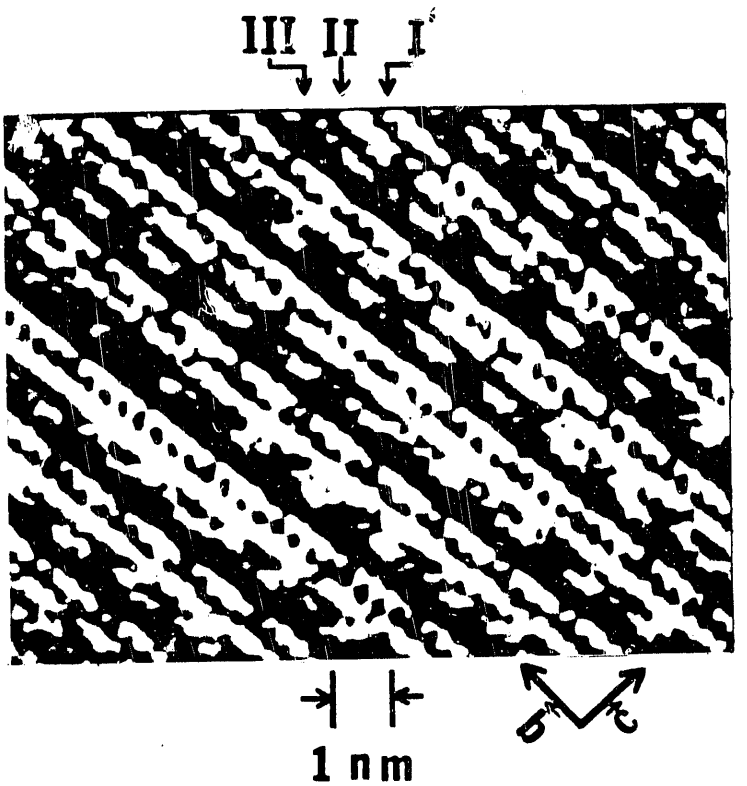

Fig. 4(a)

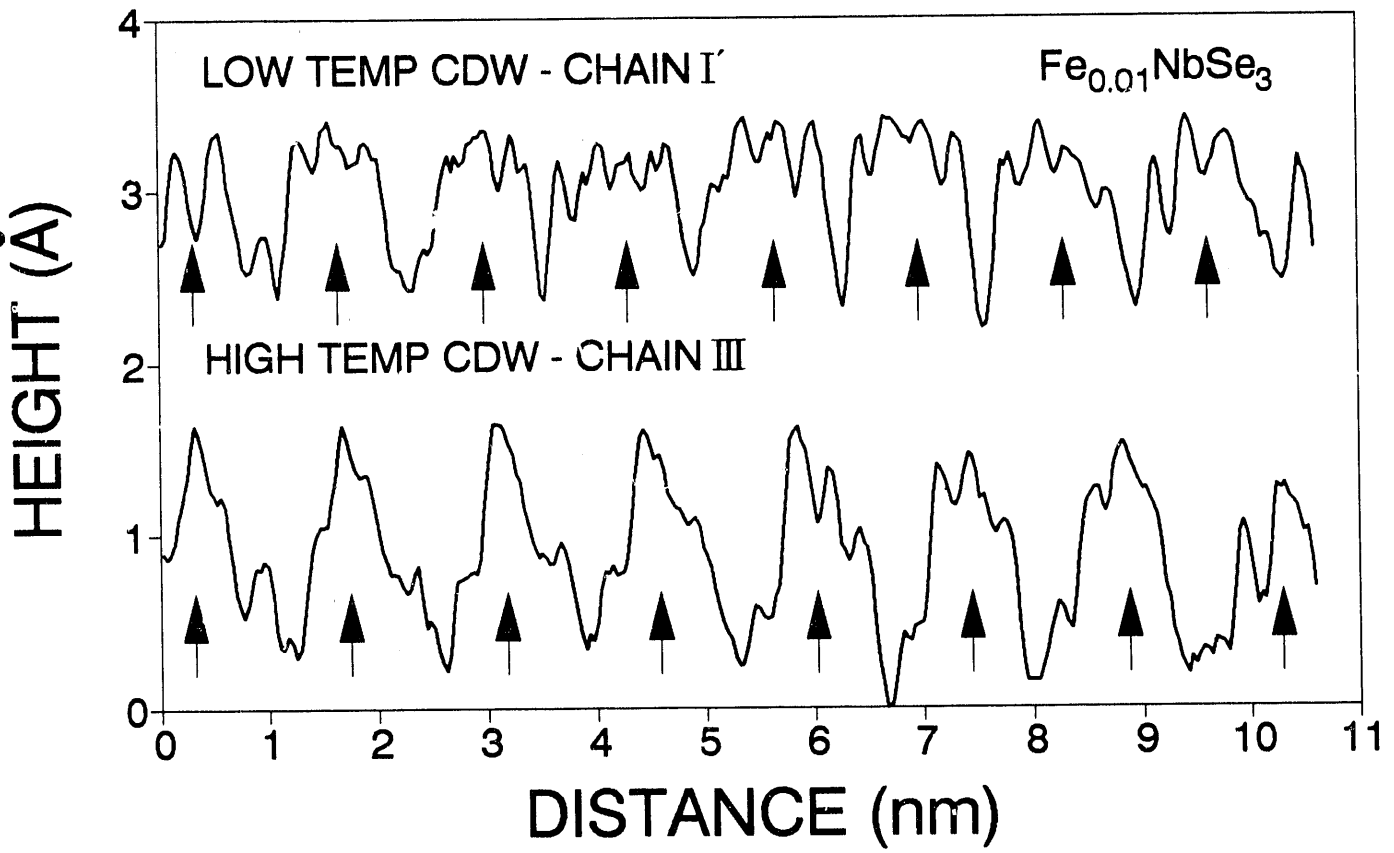
LOW TEMP CDW - CHAIN I´
$Fe_{0.01}NbSe_3$
HIGH TEMP CDW - CHAIN III
HEIGHT (Å)
DISTANCE (nm)
0
1
2
3
4
5
6
7
8
9
10
11

Fig. 4(b)

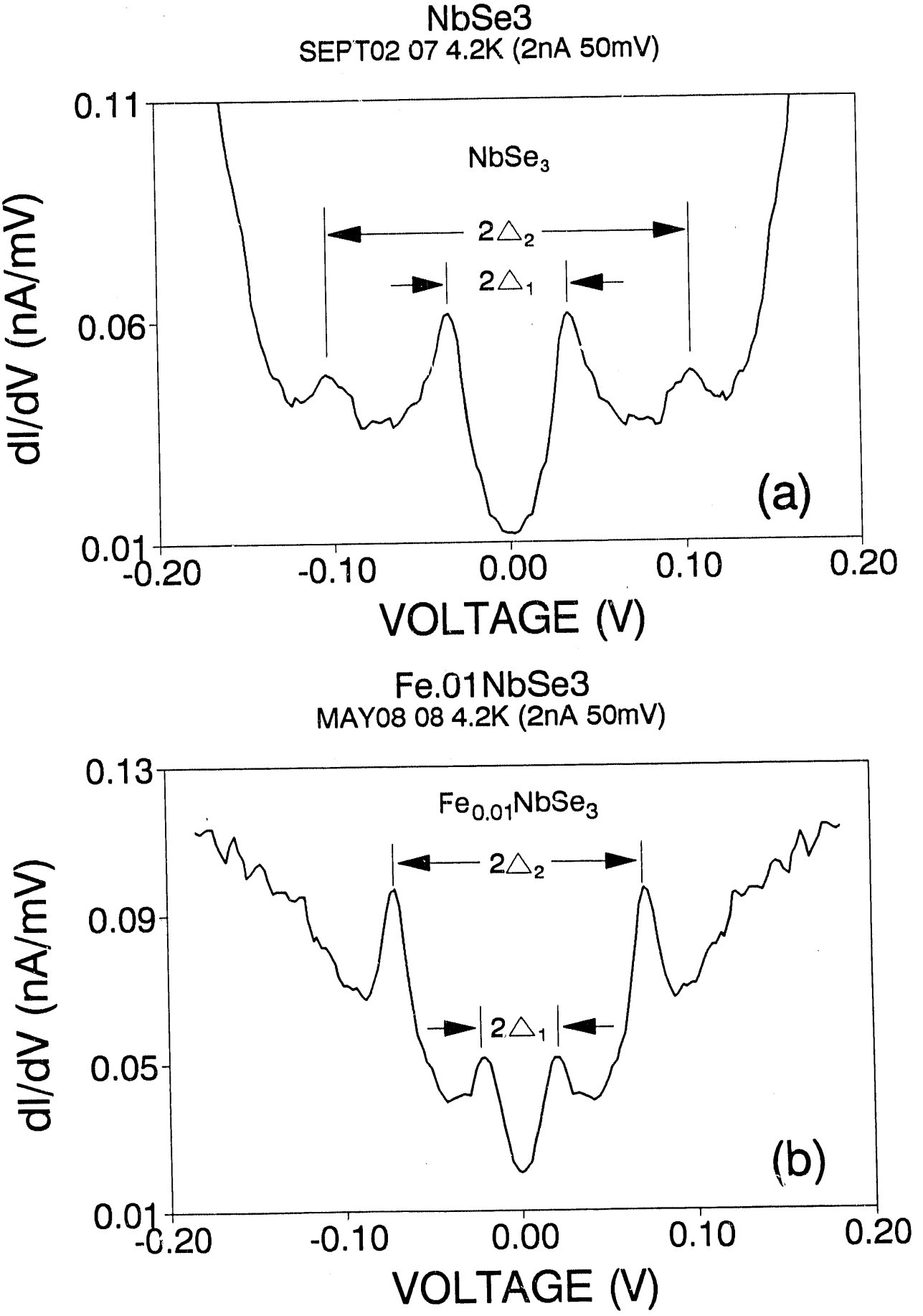
NbSe3
SEPT02 07 4.2K (2nA 50mV)
0.11
0.06
0.01
dI/dV (nA/mV)
NbSe3
2△2
2△1
(a)
-0.20
-0.10
0.00
0.10
0.20
VOLTAGE (V)
Fe.01NbSe3
MAY08 08 4.2K (2nA 50mV)
0.13
0.09
0.05
0.01
dI/dV (nA/mV)
Fe0.01NbSe3
2△2
2△1
(b)
-0.20
-0.10
0.00
0.10
0.20
VOLTAGE (V)

Fig. 5

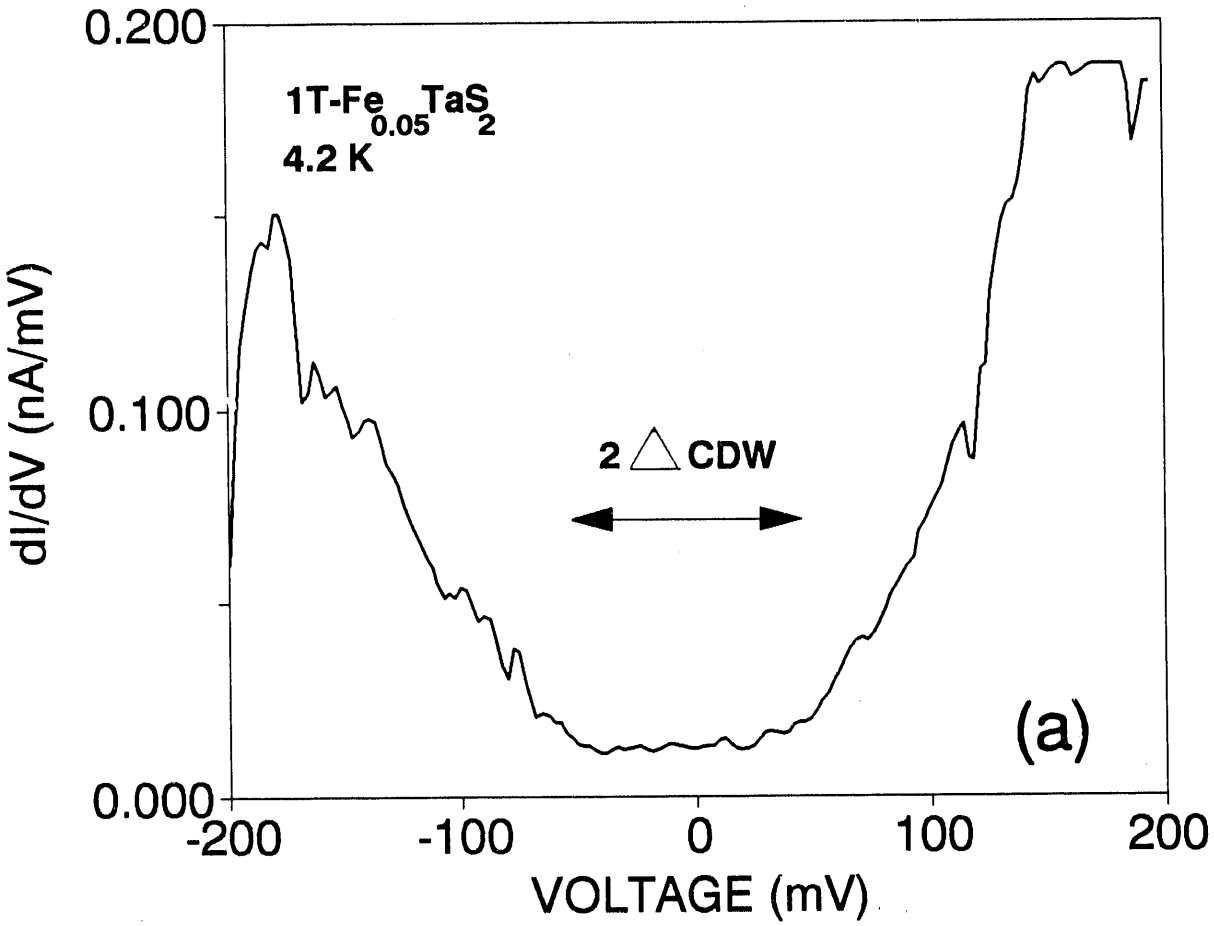
0.200
0.100
0.000
dI/dV (nA/mV)
1T-Fe0.05TaS2
4.2 K
2△CDW
(a)
-200
-100
0
100
200
VOLTAGE (mV)

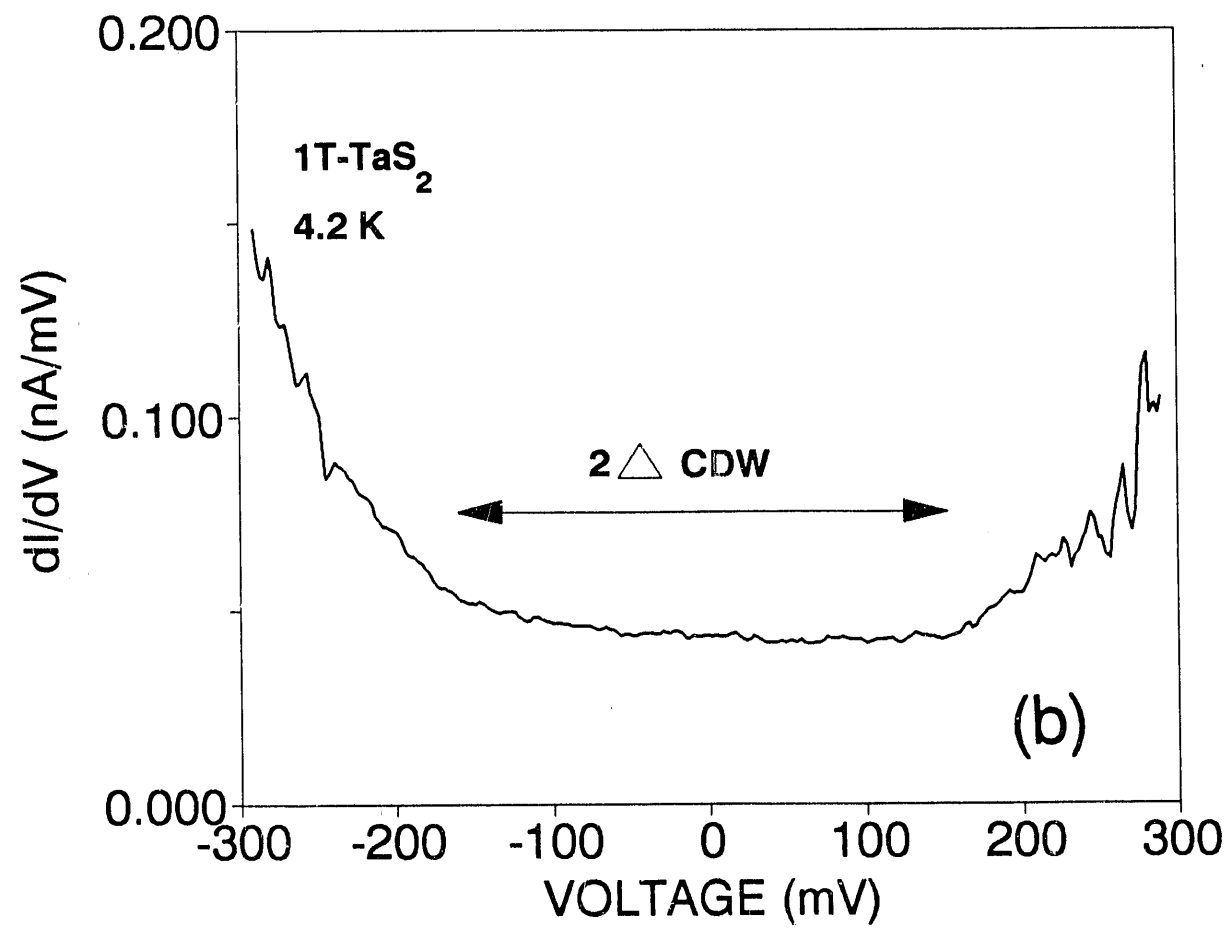
0.200
0.100
0.000
dI/dV (nA/mV)
1T-TaS2
4.2 K
2△ CDW
(b)
-300
-200
-100
0
100
200
300
VOLTAGE (mV)

Fig. 6

END

DATE FILMED

3/18/92